High Brightness Semiconductor Lasers as Transmitters for Space Lidar Systems

I. Esquivias , G. Ehret , M. Quatrevalet , A. Pérez-Serrano . J.M.G. Tijero , M. Faugeron , F. van Dijk , M. Krakowski , G. Kochem , M. Traub , J. Barbero , P. Adamiec , X. Ai , and J. Rarity

Abstract— **High brightness semiconductor lasers are potential transmitters for future space lidar systems. In the framework of the European Project BRITESPACE, we propose an all-semiconductor laser source for an Integrated Path Differential Absorption lidar system for column-averaged measurements of atmospheric CO_2 in future satellite missions. The complete system architecture has to be adapted to the particular emission properties of these devices using a Random Modulated Continuous Wave approach. We present the initial experimental results of the InGaAsP/InP monolithic Master Oscillator Power Amplifiers, providing the ON and OFF wavelengths close to the selected absorption line around 1572 nm.**

Keywords—Differential Absorption lidar; atmospheric sensing; Integrated Path Differential Absorption; Random Modulation CW lidar; semiconductor laser.

I. INTRODUCTION

Space-borne lidar systems require laser transmitters with very good performance in terms of output power, beam quality, conversion efficiency, long term reliability and environmental compatibility. Atmospheric gas sensing additionally requires spectral purity and stability. Solid state lasers are considered the most mature technology for space lidar applications, at expenses of a relatively large size and low conversion efficiency. Fiber lasers present very high power levels and very good beam quality, but the problem of their radiation sensitivity is still not solved. Recently, a new generation of high brightness semiconductor lasers based on tapered geometry has demonstrated relatively high average power levels together with a good beam quality [1-5]. These devices are emerging candidates for its direct use in space lidar systems.

Semiconductor lasers have clear advantages over other laser types in terms of compactness and conversion efficiency (up to 75%). They present high reliability and good radiation hardness for most space applications. They can be fabricated with emission wavelengths ranging from Ultra-Violet up to Far-Infrared, and those with appropriate design can be tuned over several tenths of nanometers. Broad Area lasers can achieve more than 20 W CW, but they suffer from a poor beam quality. Tapered semiconductor lasers [1-4], also known as flared unstable cavity lasers, have demonstrated both high power and good beam quality at different wavelengths. These devices consist of a ridge waveguide (RW) section and a tapered section. The single spatial mode of the RW section is launched into the tapered section where it is amplified while keeping its single mode profile. Improved epitaxial structures, together with the use of long cavity designs have led to single-emitter tapered lasers providing more than 10 W with a low beam propagation ratio M^2 at 980 nm [4] and 1060 nm [3]. The spectral properties of tapered lasers are similar to those of BA lasers, with multiple modes and broad and unstable emission spectra, but they can be enhanced by the use of a Distributed Bragg Reflector (DBR) to select a single longitudinal mode [4]. The integrated Master Oscillator Power Amplifier (MOPA) architecture, consisting of either a Distributed Feedback (DFB) or a DBR laser as oscillator and a tapered semiconductor amplifier, present advantages for those lidar applications requiring good spectral properties. Integrated DBR MOPAs have demonstrated up to 12 W in CW operation at 1064 nm [5], and DFB based MOPAs are commercially available at different wavelengths [6].

Most of lidar systems are based in high peak power pulses with a low repetition rate, but the maximum peak power of semiconductor lasers is quite limited in comparison with Solid State or Fiber lasers. Quasi-CW lidar systems are more appropriate to take advantage of the modulation properties of these devices. Random-modulation CW (RM-CW) lidar [7, 8] is capable of obtaining range gated back-scattering information as obtained from pulsed techniques.

In the framework of the European Project BRITESPACE [9] we are developing an integrated MOPA emitting at 1572 nm to be used as the source for an Integrated Path Differential Absorption (IPDA) lidar for column-averaged measurements of atmospheric CO_2 in future space missions [10]. Here we present the operation principles, the design of the complete system and the experimental results obtained to date regarding the laser transmitter.

II. SYSTEM DESIGN

A. Random-Modulation Continuous-Wave Lidar

Pulsed Integrated Path Differential Absorption (IPDA) lidar systems, such as the CO_2 and CH_4 Atmospheric Remote Monitoring-Flugzeug (CHARM-F) [11] estimate the column concentration of greenhouse gases in the atmosphere by looking at the back-scattered pulse echoes at the end of the optical path, which is either the cloud top or the Earth's surface. The term 'differential absorption' refers to the difference of the absorption of a pair of laser lines with slightly different wavelengths: the on-line wavelength (λ_{On}) is near the center of a CO_2 absorption line while the off-line

wavelength (λ_{Off}) is set close to but off the same absorption line. Both wavelengths are close enough such that the two lines exhibit almost identical aerosol attenuation but obviously different CO_2 absorption. Hence, the relative absorption by the CO_2 molecules can be calculated by the power ratio of the back-scattered signals at the end of the optical path and it can be converted into a column-averaged mixing ratio thanks to the knowledge of the path length from the round-trip time delay.

Random-modulation CW (RM-CW) lidar [7] is capable of obtaining range gated back-scattering information as obtained from pulsed techniques. In RM-CW lidar, a Pseudo-Random Binary Sequence (PRBS) is transmitted (See Fig. 1 (a)). The received signal correlated with the original PRBS code gives a range resolved response with a non-ambiguous range determined by the number of PRBS bits (repetition rate) which can be extended further than the trip time corresponding to the atmosphere thickness. The auto-correlation property of the PRBS and the temporal shifting of the codes can be used to transmit both wavelengths simultaneously, which avoids the beam misalignment problem. Fig. 1 (b) shows an example of the cross-correlation between the received signal and the emitted PRBS. The ratio between the cross-correlation intensities of the reference output and received signals provides information about the differential absorption optical depth and hence on the dry air mixing ratio of CO_2. Furthermore, due to the extended non-ambiguity distance, equals to the total PRBS code length, the returns can be binned into different range gates with the distance resolution limited by the PRBS bit time (chip time).

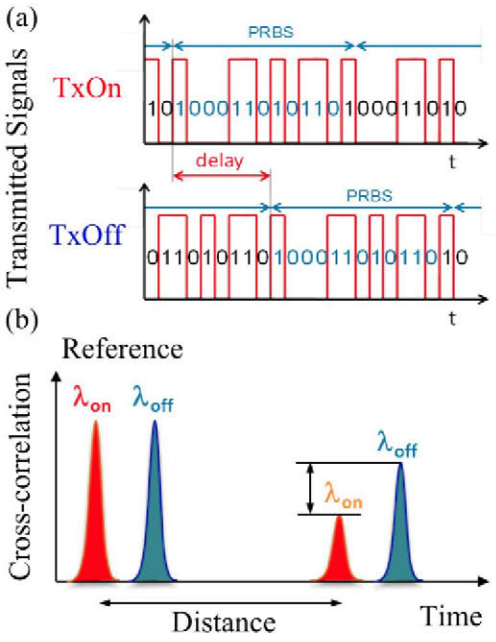

Fig. 1. Illustration of the RM-CW lidar technique. (a) Transmitted PRBS signals. (b) Cross-correlation between the emitted PRBS and the received signals allowing distance and differential absorption measurements.

B. *Lidar System*

The design of the complete IPDA lidar system is shown in Fig. 2. It consists of the laser transmitter, the optics for beam transmission and reception and the control electronics. Specifically, the output beam from the transmitter is split in two branches: one is sent to the beam expander and then to the atmosphere and the other is used as reference in the comparison with the received signal, for the calculation of CO_2 concentration. The reflected light from Earth ground is collected by a reflective telescope with a Field of View (FOV) matching the laser beam divergence and alignment issues are addressed by using a Short Wave Infrared (SWIR) camera.

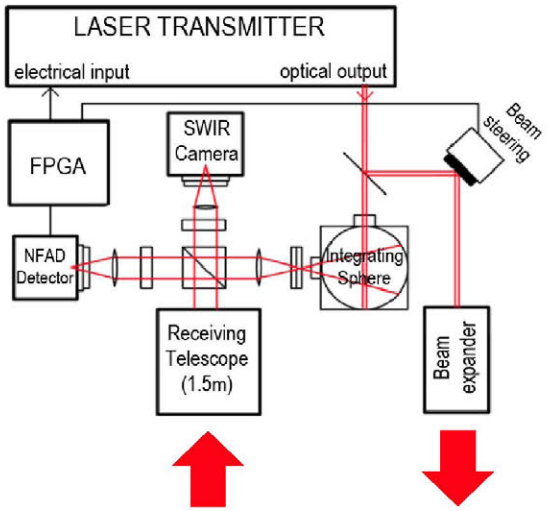

Fig. 2. Block scheme of the complete IPDA lidar system.

The main drawback of the proposed RM-CW IPDA system is the degradation of the Signal to Noise Ratio (SNR) in comparison with pulsed systems due to the ambient and detector noise [12]. This effect can be minimized by using a narrow spectral filter at the receiver and by optimizing the detector characteristics. A very high sensitivity detector based on InGaAs Negative Feedback Avalanche Diodes (NFAD) is proposed for single photon counting of the received signal [12]. The modulation sequence and the correlation process required by the RM-CW technique are implemented with a Field Programmable Gate Array (FPGA).

III. Laser Transmitter

The laser transmitter architecture is shown in Fig. 3. It consists of two space compatible laser sub-modules, the control electronics and the Frequency Stabilization Unit (FSU). Two laser chips, one for each sounding frequency (λ_{On}, λ_{Off}) required for CO_2 detection in IPDA systems, are housed in the laser module, together with the beam forming optics and two power monitoring photodiodes. The back facet output of the laser chips are sent to the FSU through standard Single Mode Fibers (SMF) for frequency stabilization.

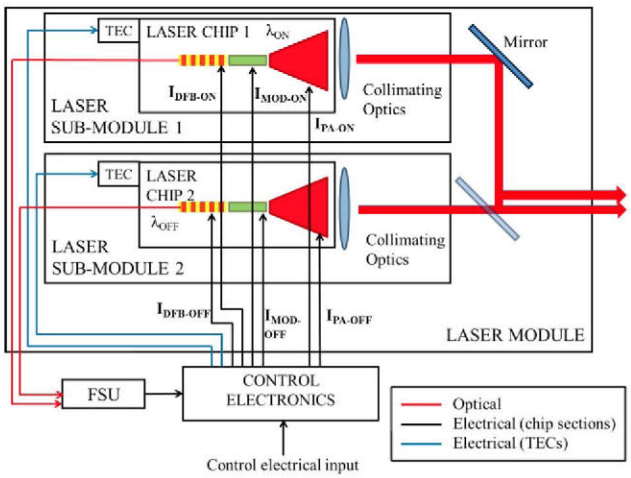

Fig. 3. Block scheme of the laser transmitter.

A. *Laser Module*

For each laser chip, a sub-module has been designed in order to provide electrical access, temperature control and beam forming optics for each tapered MOPA. Fig. 4 (a) shows the design of the laser module; Fig. 4 (b) shows a photograph of a real sub-module with a working MOPA without the collimating optics. The radiation emitted by the tapered amplifier is astigmatic, i.e. it has different virtual sources (and different angles of divergence) for the fast axis (vertical direction) and for the slow axis (horizontal direction). Due to this characteristic an optical system for the collimation of a tapered amplifier must consist of two lenses.

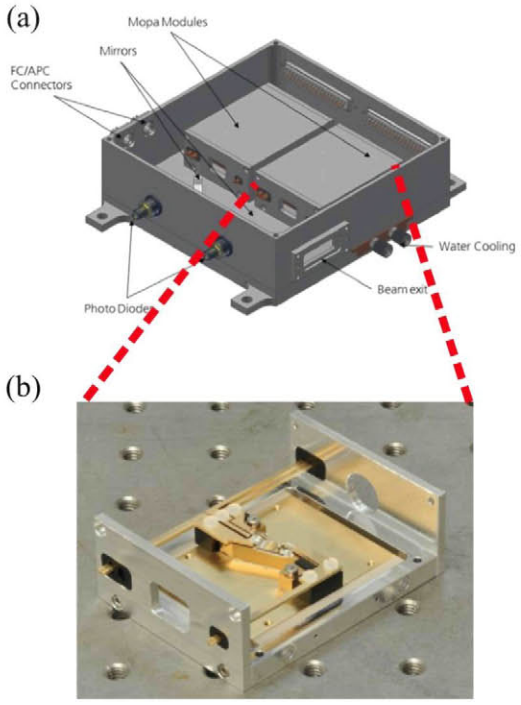

Fig. 4. (a) Design of the laser module. (b) Photograph of the laser sub-module without the collimating optics.

We propose the use of a first aspheric lens and a second cylindrical lens. The first lens is for collimation of the fast axis and intermediate focusing of the slow axis while the second cylindrical lens collimates the slow axis without affecting the fast axis beam. Considering also the bended geometry of the laser chips, the emitter is tilted in the slow axis in order to achieve perpendicular propagation.

The radiation emitted from the back facet of the DFB is expected to be diffraction limited, and therefore can be coupled into a lensed Single Mode Fiber (SMF) aligned to the DFB back facet.

Two mirrors, one for each sub-module, are used for combining the output beams before exiting the laser module. Partially reflective mirrors will be used in order to allow power monitoring for each MOPA with two photodiodes placed right after the combining mirrors. The laser beams from the two laser chips are placed close each other at the laser module output, for minimizing footprint errors in IPDA detection.

B. *Frequency Stabilization Unit*

For accurate estimation of gas molecule concentration IPDA lidar systems require high frequency stabilization, in order to have precise measurement of the detected power ratio at the selected absorption line [10]. In our case, the proposed absorption line is at 1572 nm. It has been chosen because of its high absorption and low interference from the H_2O lines.

Regarding frequency stability and knowledge accuracy, the most critical is the on-line frequency, due to the slope in the wing of the line. The linewidth and linewidth knowledge accuracy is expected to be uncritical for the BRITESPACE transmitter, because pseudo-random modulation dominates the linewidth which is therefore well known.

In order to achieve these frequency requirements, we use two opto-electrical feedback loops for the stabilization of the on- and off-channels coupled to the output of a third opto-electrical feedback loop for CO_2 locking.

Light emitted from the back facet of the DFB section of the on-line MOPA is collected through a lensed SMF fiber and sent to a fiber coupler. One of the output ports of the coupler will be sent to the on-line locking feedback loop and the other will be used for monitoring. In the same way, the light emitted from the back facet of the off-line MOPA will be sent to a second fiber coupler. One of the outputs will be sent to the off-channel locking feedback loop while the other will be used for monitoring.

We will use a master DFB laser that will be locked to the selected CO_2 absorption line using a multi pass CO_2 reference cell and a custom feedback loop based on a commercially available laser frequency locking equipment. The light emitted from the master laser will be injected into the on- and off-line frequency locking loops and it will be used to stabilize the beat note of the on- and off-line signals with respect to the master laser frequency, with a tunable 350 MHz and with a fixed 10 GHz offsets, respectively.

C. Laser Chip

InGaAsP/InP monolithic MOPAs were fabricated as the main building block of the laser transmitter. Each MOPA is a three section device, consisting of a frequency stabilized DFB master oscillator, a modulator section, and a tapered Semiconductor Optical Amplifier (SOA). The use of this original structure aims to fulfill the performances required by the IPDA system in terms of high power, frequency stability and good beam quality. The DFB section is accurately frequency stabilized by an external opto-electrical feedback loop through the FSU. The modulator section is introduced for implementation of the RM-CW technique in the proposed IPDA system. Finally, the geometry of the tapered SOA is optimized in order to provide high brightness output beam with sufficient power and beam quality.

We have designed our asymmetrical cladding structure using a dilute slab composed of InP and InGaAsP (λ_g = 1.17 µm) in order to avoid any material development. Indeed this quaternary material is the same as the barrier material. The slab thickness (1.62 µm) has been optimized to decrease the optical confinement within the p-doped layers as much as possible and to maintain the confinement within the Quantum Wells (QWs) around 2%. This level of confinement is necessary to maintain a low threshold current, a low RIN and a quite large relaxation frequency.

The multiple QWs DFB structure was grown by Metal Organic Chemical Vapor Deposition (MOCVD) on n-InP substrates. The active region contains six 8 nm thick compressively (0.85%) strained InGaAsP quantum wells and five 10 nm thick InGaAsP (λ_g = 1.17 µm) barriers. The photoluminescence peak was 1.57 µm. After a first epitaxy, first order gratings were defined by e-beam lithography and inductively coupled plasma (ICP) reactive ion etching. The InGaAsP grating layer is positioned above the active zone and the grating layer thickness is optimized in order to obtain a coupling strength KL ~ 1.4. This low value of KL should limit spatial hole burning and the associated optical power saturation. Re-growth of p-doped top cladding was then also done by MOCVD. The ridge-waveguides are 3.0 µm wide. This value was found to minimize the thermal saturation while preserving lateral single-mode operation. Bars were cleaved to form 4 and 5 mm long devices. Facets were high reflectivity (HR) coated on the DFB laser backside facet and antireflection (AR) coated on the SOA facet. Chips cleaved from the bars were mounted p-side up on aluminum nitride (AlN) sub-mounts. A thermistor was glued on the sub-mount to better control the chip temperature.

Three different geometries were initially proposed and fabricated for the laser chip implementation, based on i) straight, ii) tilted, and iii) bended designs. The tilted and bended geometries were proposed in order to minimize undesired optical feedback from the amplifier section to the DFB oscillator. In fact, standard straight monolithically integrated MOPAs exhibit instabilities due to compound cavity effects arising from the residual reflectivity at the amplifier output facet [13, 14]. In order to decrease the reflections at the facets, a simple method consists in tilting the device with regard to the facets. This technique is very common for SOAs. The main drawback is the difficulty to make efficient high reflective coatings on the backside DFB laser facet due to the tilt.

The best experimental results in terms of output power and spectral quality were obtained for the bended geometry shown in Fig. 5 (a). Fig. 5 (b) shows a photograph of the bended MOPA where the different contacts for the three sections and the thermistor contact for temperature control can be observed.

The measurements have been done on a device mounted on AlN sub-mounts. The current was injected through electrical probes for the DFB laser and the modulator and trough large metallic stripes for the flared SOA in order to reduce the electrical resistance and to allow high current values. The sub-mount temperature was controlled thanks to the thermistor glued on the sub-mount. All the measurements have been performed at 18° C.

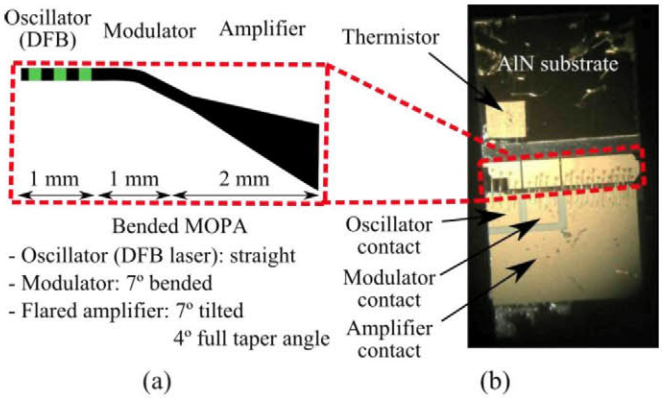

Fig. 5. (a) Scheme of the bended MOPA. (b) Photograph of the bended MOPA showing the contacts of each section.

The measured CW output power vs. amplifier current characteristics for a bended MOPA are shown in Fig. 6 for different modulator section currents and a fixed DFB current of 400 mA. The maximum optical power of around 400 mW corresponds to a modulator current of 300 mA. The static Extinction Ratio (ER) when switching the modulator current between 0 and 300 mA is 26 dB.

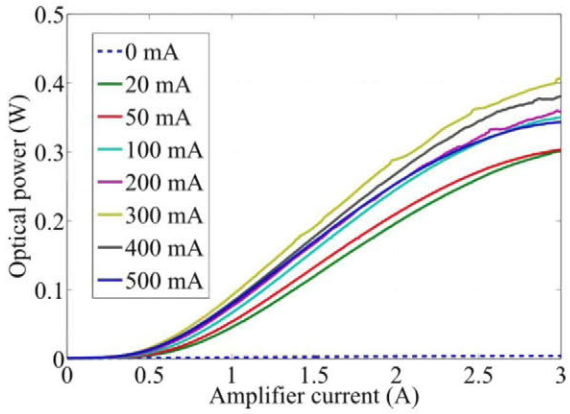

Fig. 6. Experimental L-I curves of the bended MOPA for different values of the modulator current. The pump current of the oscillator (DFB) is fixed to 400 mA.

Fig. 7 (a) shows the optical spectra for different modulator currents. The emission wavelength around 1583 nm, higher than the target wavelength, but this will be corrected in next fabrication runs. Single frequency operation with Side Mode Suppression Ratio (SMSR) around 50 dB is apparent. The peak wavelength shows high stability when changing the modulator current, with a maximum shift of 40 pm, as it can be observed in Fig. 7 (b). This shift is attributed to cross-heating effects in static conditions, but it is not expected at the proposed modulation rate of 25 Mbps.

The output power is limited by the flared SOA thermal saturation. This saturation appears at low current density (2 kA.cm^{-2}) compared with similar structures such as [15] (4.64 kA.cm^{-2}). We think this limitation is due to fabrication issues during the p-side contact annealing. Higher power levels are expected in next fabrication runs.

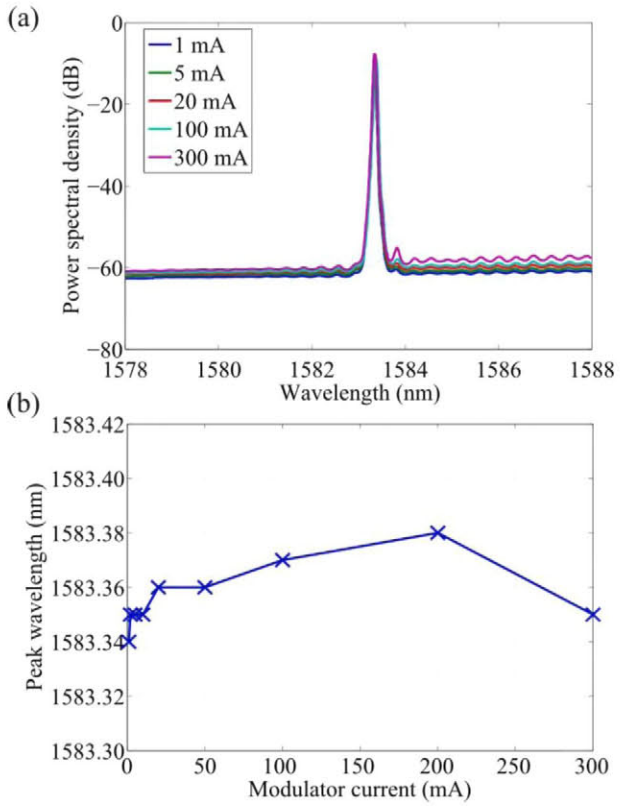

Fig. 7. (a) Optical spectra for different current values of the modulator section. The pump current of the oscillator (DFB) is fixed at 400 mA, while the pump current of the amplifier is fixed at 3 A. (b) Peak wavelength of the optical spectra shown in (a) for the different modulator currents.

IV. Summary

In this paper, we report on the progresses of the BRITESPACE Consortium in order to achieve space-borne lidar measurements of atmospheric carbon dioxide concentration based on an all semiconductor laser source at 1.57 µm. The complete design of the proposed RM-CW IPDA lidar has been presented and described in detail. Complete descriptions of the laser module and the FSU have been presented. Two bended MOPAs, emitting at the sounding frequency of the on- and off- IPDA channels, have been proposed as the transmitter optical sources with the required high brightness.

We have demonstrated more than 400 mW output power with a SMSR higher than 45 dB and stable emission. Experimental results on the bended MOPAs have been presented showing a high spectral purity and promising expectations on the high output power requirements.

Acknowledgment

This work was supported by the European Commission through the project BRITESPACE under grant agreement no. 313200.

References

[1] J.N. Walpole, "Semiconductor amplifiers and lasers with tapered gain regions," Opt. Quantum Electron., vol. 28, pp. 623-645, 1996.

[2] H. Wenzel, B. Sumpf, G. Erbert, "High-brightness diode lasers," C. R. Physique, vol. 4, pp. 649-661, 2003.

[3] B. Sumpf, et al., "High-Brightness Quantum Well Tapered Lasers," IEEE J. Selected Topics Quantum Electron., vol. 15, pp. 1009-1020, 2009.

[4] C. Fiebig, et al., "High-Power DBR-Tapered Laser at 980 nm for Single-Path Second Harmonic Generation," IEEE J. Select. Topics Quantum Electron. vol. 15, pp. 978-983, 2009.

[5] H. Wenzel, et al., "High peak power optical pulses generated with a monolithic master-oscillator power amplifier," Opt. Lett., vol. 37, pp. 1826-1828, 2012.

[6] http://www.qpclasers.com/

[7] N. Takeuchi, N. Sugimoto, H. Baba, and K. Sakurai, "Random modulation cw lidar," Appl. Opt., vol. 22, pp. 1382-1386, 1983.

[8] X. Ai, R. Nock, J.G. Rarity, and N. Dahnoun, "High-resolution random-modulation cw lidar," Appl. Opt., vol. 50, pp. 4478-4488, 2011.

[9] http://www.britespace.eu/

[10] G. Ehret, et al., "Space-borne remote sensing of CO2, CH4, and N2O by integrated path differential absorption lidar: a sensitivity analysis," Appl. Phys. B, vol. 90, pp. 593-608, 2008.

[11] M. Quatrevalet, et al., "CHARM-F: The airborne integral path differential absorption lidar for simultaneous measurements of atmospheric CO2 and CH4," in Proc. 25th Int. Laser Radar Conf., St. Peterburg, Russia, 2010.

[12] X. Ai et al., "Pseudo-random single photon counting for space-borne atmospheric sensing applications" in IEEE Aerospace Conference, Big Sky, Montana, USA, 2014.

[13] M. Spreemann, M. Lichtner, M. Radziunas, U. Bandelow, and H. Wenzel, "Measurement and simulation of distributed feedback tapered master-oscillator power-amplifiers" IEEE J. Quantum Electron., vol. 45, pp. 609–616, 2009.

[14] P. Adamiec, B. Bonilla, A. Consoli, J. M. G. Tijero, S. Aguilera, and I. Esquivias, "High-peak-power pulse generation from a monolithic master oscillator power amplifier at 1.5 µm," Appl. Opt., vol. 51, pp. 7160-7164, 2012.

[15] L. Hou, M. Haji, J. Akbar, and J. H. Marsh, "Narrow linewidth laterally coupled 1.55 µm AlGaInAs/InP distributed feedback lasers integrated with a curved tapered semiconductor optical amplifier," Opt. Lett., vol. 37, no. 21, pp. 4525-4527, Nov., 2012.